HHS Public Access

Author manuscript

Brain Res. Author manuscript; available in PMC 2021 January 15.

Published in final edited form as:

Brain Res. 2020 January 15; 1727: 146552. doi:10.1016/j.brainres.2019.146552.

Functional Brain Activity Is Globally Elevated by Dopamine D2 Receptor Knockdown in the Ventral Tegmental Area

Tamriage A. Martin, **Hilary R. Smith**, **Deborah J. Luessen**, **Rong Chen**, **Linda J. Porrino***

Department of Physiology and Pharmacology, Wake Forest School of Medicine, Winston-Salem, NC 27157

Abstract

The mesocorticolimbic system is comprised of dopaminergic neurons in the ventral tegmental area (VTA) and their projection targets in the ventral striatum, amygdala, prefrontal cortex, and hippocampus, among others. Regulation of dopamine transmission within this system is achieved in part through a negative feedback mechanism via dopamine D2 autoreceptors located on somatodendrites and terminals of VTA dopaminergic neurons. Dysregulation of this mechanism has been implicated in addiction and other psychiatric disorders, although the biological bases for these associations are unclear. In order to elucidate the functional consequences of VTA D2 receptor dysregulation, this study investigated alterations in local cerebral glucose utilization throughout the brain following *Drd2* knockdown in the VTA.

Male Sprague-Dawley rats received bilateral injections of lentivirus encoding shRNAs against the rat dopamine D2 receptor, scrambled shRNA or phosphate buffered saline. The autoradiographic 2-[^{14}C]deoxyglucose metabolic mapping procedure was conducted 22 days post-infection. Brains were sectioned for autoradiography and glucose utilization was measured across distinct regions throughout the brain.

Local cerebral glucose utilization was found to be elevated in the *Drd2* knockdown group as compared to control groups. These greater levels of metabolic activity following *Drd2* knockdown in the VTA were observed not only in the mesocorticolimbic system and associated dopamine pathways, but also in a global pattern that included many areas with far less concentrated VTA dopamine inputs. This suggests that even a partial *Drd2* deletion in the VTA can have widespread consequences and impact information flow in diverse networks that process sensory, cognitive, motor and emotional information.

Keywords

Dopamine D2 autoreceptors; Mesocorticolimbic system; Ventral tegmental area; D2 receptor knockdown; Local cerebral glucose utilization

***Corresponding Author:** Linda J. Porrino, Ph.D., Department of Physiology & Pharmacology, Wake Forest School of Medicine, Medical Center Blvd., Winston-Salem, NC 27157, lporrino@wakehealth.edu, Phone: 336-716-8590, Fax: 336-716-8501.

Declarations of interest: none.

1. Introduction

Dopamine neurons in the ventral tegmental area and their projections are thought to be essential for processes involving motivation, reward signaling, stimulus salience, and reward prediction error (Hikosaka et al., 2008; Koob, 1996; Robbins, 2003; Salamone and Correa, 2012; Schultz, 2015). Dysregulation of VTA dopaminergic function has been implicated in many neuropsychiatric disorders including addiction, depression, and schizophrenia (Grace, 2016; Koob and Volkow, 2010; Nestler and Carlezon, 2006; Nutt et al., 2015). Neurons in the VTA have widespread connections throughout the brain that extend both rostrally and caudally. Numerous studies that date back to the development of histofluorescence methods (see, for example, Anden et al., 1966; Fallon and Moore, 1978; Lindvall and Bjorklund, 1974) demonstrated projections from the VTA to the striatum and other forebrain structures. With the use of additional anatomical techniques, the projection fields of the VTA have been shown to include among others the nucleus accumbens, olfactory tubercle, prefrontal and cingulate cortex, ventral pallidum, amygdala, thalamus, septum, bed nucleus of the stria terminalis, hippocampal formation, raphe nuclei and cerebellum (Beckstead et al., 1979; Gasbarri et al., 1994a, 1994b; Ikai et al., 1992; Klitenick et al., 1992; Swanson, 1982; Thierry et al., 1973). Thus, the VTA has a very broad projection network that may help to explain the extent and diversity of its impact on behavior.

Dopamine signaling in this system is thought to be achieved through two families of receptors: D1-like receptors, including D1 and D5 subtypes, and D2-like receptors, including D2, D3, and D4 subtypes. Based on cellular localization and functionality, D2 receptors are categorized into two subtypes: postsynaptic dopamine D2 receptors and dopamine D2 autoreceptors. The majority of D2 receptors are found on postsynaptic neurons in dopaminergic terminal fields where they integrate information from a variety of neuronal circuits. In contrast, D2 autoreceptors are expressed in the somatodendritic compartments of midbrain dopaminergic neurons in the VTA and substantia nigra and presynaptically on the dopamine neurons projecting to mesolimbic, mesostriatal and prefrontal cortical structures. The D2 autoreceptors primarily regulate dopaminergic signaling through negative feedback inhibition of dopamine cell excitability and the synthesis and release of dopamine (for reviews see Beaulieu and Gainetdinov, 2011; Ford, 2014).

In rodent models, deficits in D2 autoreceptors have been linked to greater vulnerability to cocaine acquisition and heightened cue reactivity (Holroyd et al., 2015), increased motivation to self-administer (de Jong et al., 2015), and greater sensitivity to the acute locomotor and rewarding effects of cocaine (Bello et al., 2011); these effects were attributed to the loss of feedback inhibition of D2 autoreceptors on dopamine neuron excitability and presynaptic dopamine release. Similarly, our group has previously shown that even a moderate reduction of D2 receptors in the VTA achieved through lentiviral knockdown results in increased vulnerability to cocaine self-administration (Chen et al., 2018), while others using similar approaches have shown increased impulsivity as measured by a delay discounting task (Bernosky-Smith et al., 2018). In humans, the role of midbrain D2 receptors has been examined using positron emission tomography (PET) imaging of dopamine receptor availability (Buckholtz et al., 2010; Dang et al., 2018; Zald et al., 2008,

2010). These studies have demonstrated a wide range of variability in midbrain D2 receptor availability across normal volunteers and patient populations. Furthermore, these investigators reported that basal midbrain D2 receptor availability was correlated with measures of impulsivity, novelty seeking, and reward valuation (Buckholtz et al., 2010; Dang et al., 2018; Zald et al., 2008).

These studies in rodents and humans examining midbrain dopamine D2 receptors have largely focused on the effects of changes in receptor function on dopamine dynamics in the striatum. There has been far less consideration of the consequences of alterations in VTA D2 receptors in other brain areas. Thus, the purpose of the present study was to investigate the effects of the reduction of dopamine D2 receptors in the VTA on functional brain activity throughout the entire brain, including both those areas that receive direct projections from the VTA as well as other brain areas with sparse or no known direct VTA dopamine innervation. To this end we employed a D2 receptor knockdown model that has previously been shown to reduce VTA *Drd2* mRNA expression levels in rats by approximately 30% using lentivirus encoding *Drd2* shRNAs (Chen et al., 2018). The quantitative autoradiographic 2-[^{14}C]deoxyglucose (2-DG) method was then used to measure glucose utilization throughout the brain of *Drd2* knockdown and corresponding control animals.

2. Results

2.1 Verification of injection sites and viral infection

The lentivirus encoding *Drd2* shRNA to knock down midbrain dopamine D2 receptors was validated as previously described (Chen et al., 2018). The *Drd2* mRNA in the VTA was shown to be reduced in average by 30% and this reduction was persistent for 6 months. Because the lentivirus also encodes the green fluorescent protein (GFP) gene, immunofluorescence staining was performed to assess the localization of GFP in dopamine neurons by examining the co-localization of GFP with tyrosine hydroxylase (TH), a marker for dopaminergic neurons. As shown in Figure 1, GFP fluorescence signal was predominantly localized in TH-positive VTA dopaminergic neurons, suggesting that the lentivirus effectively infected dopaminergic neurons. As indicated by the presence of some TH-/GFP+ cells, however, a small portion of infected neurons were not dopaminergic. Three animals in which injections were misplaced were excluded from further analysis.

2.2 Local Cerebral Glucose Utilization

Rates of local cerebral glucose utilization were measured in three experimental groups: D2 receptor knockdown (*Drd2KD*), scrambled shRNA control (SCR), and phosphate buffered saline control (PBS). A total of 34 brain regions were analyzed, and the results are reported in Table 1 and Figure 2. Global rates of cerebral metabolism in the *Drd2KD* group (88.8 ± 3.27) were significantly higher than those of the SCR (72.4 ± 3.74) or PBS (75.0 ± 4.94) animals; one way ANOVA ($F_{(2,18)} = 5.771$, $p < 0.01$) followed by Bonferroni multiple comparisons, $p < 0.05$. It is important to note that there were no differences in global rates of cerebral metabolism between the two control groups (SCR and PBS), thus providing evidence that the virus itself does not alter glucose utilization. Data from specific brain regions are described in detail below.

2.2.1 Mesolimbic—As shown in Table 1, within the mesolimbic system, which includes those areas which receive direct projections from the VTA, there were significant main effects of treatment ($F_{(1,19)}$= 12.12, p <.005) and brain region ($F_{(6,19)}$= 65.94, p <.001). Rates of glucose utilization were significantly higher in the *Drd2KD* rats as compared to rates of controls rats. Further analysis of individual brain regions revealed that rates of glucose utilization of *Drd2KD* rats were significantly higher in the rostral accumbens (+18%), accumbens core (+27%), accumbens shell (+31%), olfactory tubercle (+26%), ventral pallidum (+25%), ventral tegmental area (+19%) and lateral habenula (+19%) as compared to values of animals in the combined control groups.

2.2.2 Nigrostriatal—Analysis of rates of glucose utilization in regions within the nigrostriatal system (Table 1) showed significant main effects of treatment ($F_{(1,19)}$= 13.15, p <.005) and brain region ($F_{(7,19)}$= 342.96, p <.001), as well as a significant region X treatment interaction ($F_{(7,133)}$= 6.20, p <.001. Multiple comparisons demonstrated significantly higher rates of cerebral glucose utilization in the dorsal caudate (+24%), lateral caudate (+21%), ventral caudate (+25%), entopeduncular nucleus (+18%), subthalamic nuclei (+24%), substantia nigra compacta (+15%), and substantia nigra reticulata (+19%) of *Drd2KD* rat brain regions compared to values of animals in the combined control groups.

2.2.3 Limbic—Rates of glucose utilization for limbic-related brain regions, many of which receive VTA projections, are shown in Table 1. Statistical analysis revealed significant main effects of treatment ($F_{(1,19)}$= 11.50, p <.005) and brain region ($F_{(6,19)}$= 94.37, p <.001). Post hoc tests showed significantly higher rates of local cerebral glucose utilization in the lateral septum (+24%), medial forebrain bundle (+17%), basolateral amygdala (+19%), central amygdala (+24%), hippocampus CA1 (+22%), hippocampus CA3 (+18%), and the dentate gyrus (+23%) regions when compared to rates of animals in the combined control groups.

2.2.4 Cortex and Thalamus—Rates of glucose utilization for cortical and thalamic brain regions are shown in Table 1. Within these areas, there were significant main effects of treatment ($F_{(1,19)}$= 12.39, p <.005) and brain region ($F_{(5,19)}$= 308.42, p <.001), as well as a significant treatment X region interaction ($F_{(5,95)}$= 3.76, p <.005). Post hoc comparisons showed significantly higher rates of cerebral metabolism in the medial prefrontal cortex (+24%), anterior cingulate cortex (+22%), motor cortex (+23%), lateral thalamus (+19%), and medial thalamus (+20%) in the *Drd2*KD group as compared to values of animals in the combined control groups.

2.2.5 Brainstem—Within regions of the brainstem (Table 1), there were significant main effects of treatment ($F_{(1,19)}$= .16, p <.025) and brain region ($F_{(5,19)}$= 66.01, p <.001). Multiple comparisons showed a significantly elevated rates of cerebral glucose utilization in the locus coeruleus (+22%), habenula (+18%), and cerebellum (+19%) of *Drd2KD* rats as compared to rates of animals in the combined control groups.

3.0 Discussion

The present study demonstrated that a reduction in dopamine D2 receptor mRNA levels in the VTA produced by lentiviral gene knockdown resulted in widespread elevations in functional brain activity, as reflected by higher rates of glucose consumption measured with the 2-[^{14}C]deoxyglucose method, as compared to controls injected with either PBS saline or scrambled virus. Significant increases in functional activity were observed in those regions that receive direct dopaminergic projections from the VTA including the nucleus accumbens, olfactory tubercle, medial prefrontal cortex, ventral pallidus, lateral septum, hippocampus, habenula, and cerebellum. Within this system, not only were there large elevations in activity in the ventral striatum, where the density of dopamine inputs is highest, but also in areas with less dense dopaminergic projections when compared to the ventral striatum, e.g. the hippocampus and cerebellum, among others. In addition, increases were also noted in many other regions outside the primary projection fields of the VTA such as the globus pallidus, entopeduncular nucleus, and lateral thalamus. These data, then, suggest that even a partial reduction of dopamine D2 receptors in the VTA can have a widespread impact throughout circuits and/or networks both directly and indirectly innervated by the VTA. Although the 2-DG method is most often used to measure alterations in functional activity associated with experimental manipulations, it can also be used to assess differences in baseline brain glucose metabolism associated with different states or phenotypes, as in the present study. These widespread increases in functional activity, then, are likely the source of the alterations in behavior that have been noted after similar manipulations (Bello et al., 2011; Bernosky-Smith et al., 2018; Chen et al., 2018; de Jong et al., 2015; Holroyd et al., 2015; Linden et al., 2018).

Dopamine D2 autoreceptors control dopamine cell excitability and dopamine release via multiple mechanisms (for reviews see Beaulieu and Gainetdinov, 2011; Ford, 2014). In the midbrain autoreceptors localized on the soma and dendrites of dopamine cells inhibit neuronal excitability (Aghajanian and Bunney, 1977; Beckstead et al., 2004; Courtney et al., 2012; Lacey et al., 1987). Midbrain dopamine D2 autoreceptors directly couple to G-protein-coupled inwardly rectifying potassium (GIRK) channels via Gβγ subunits (Pillai et al., 1998). Stimulation of midbrain D2 autoreceptors opens GIRK channels, which increases the membrane potassium conductance and thus inhibits dopamine neuron firing (Beckstead et al., 2004; Lacey et al., 1987; Pucak and Grace, 1994). Somatodendritic autoreceptor-mediated inhibition of dopamine cell excitability can be generated with small spontaneous release events, and does not require burst firing or stimulated release (Gantz et al., 2013), suggesting that this component of autoreceptor function would contribute to the regulation of basal dopamine tone. Indeed, it has previously been demonstrated that basal firing rates in dopamine cells are inversely related to dopamine D2 agonist-induced suppression and antagonist-induced excitation, suggesting that cells expressing fewer or less sensitive autoreceptors exhibit greater spontaneous activity (Pucak and Grace, 1994; White and Wang, 1984). Reducing D2 autoreceptor numbers in the VTA, then, may increase basal firing rates of otherwise quiescent cells, and amplify the population activity. The current study measured LCGU under baseline conditions; the animals were in their home cages and there were no pharmacological manipulations or stimuli applied during the uptake of the 2-DG. It is likely,

then, that the observed elevations in functional activity reflect the reduction in VTA somatodendritic autoreceptors damping inhibitory control over basal dopamine tone. This heightened tone may also confer a lower threshold for phasic or burst activity due to external stimuli or pharmacological manipulation.

The autorecepter-mediated modulation of not only dopamine cell excitability, but also dopamine synthesis and release, inevitably impacts downstream signaling in the targets of the dopaminergic projections such as the striatal complex, prefrontal cortex, amygdala, and hippocampus. In fact the global nature of the increases in functional activity observed in the present study suggests that autoreceptor-associated differences in baseline dopamine transmission ultimately influence many brain networks and are not simply confined to the primary projection fields of the mesocorticolimbic system. Recent imaging studies in rodents used optogenetics to stimulate VTA dopamine neurons while simultaneously measuring brain activity with blood-oxygen-level-dependent and cerebral blood-volume-weighted functional magnetic resonance imaging. Interestingly, brain activation was not limited to the direct downstream targets of the VTA, but was also observed in areas with sparse or no VTA innervation such as the dorsal striatum, globus pallidus, and thalamus (Decot et al., 2017; Lohani et al., 2017). This influence of VTA on extra-mesolimbic targets is consistent with the current findings of widespread elevations in cerebral glucose utilization following knockdown of D2 receptors. While the abovementioned imaging studies looked at the consequences of phasic dopamine release, and the effects observed in this study were more likely the result of autoreceptor-mediated adaptations in baseline dopamine activity, they all serve to illustrate the extensive influence of the mesocorticolimbic system on the brain in general, and highlight the potential vulnerability of multiple circuits in the CNS when this system becomes dysregulated.

It is important to note that although the majority of cells in the VTA are dopaminergic, there are also many non-dopaminergic neurons that send projections to many of these same brain regions as VTA dopamine neurons (Morales and Margolis, 2017; Swanson, 1982). D2 receptors are also located on these non-dopaminergic cells in the VTA (Sesack et al., 1994). For example, it has been proposed that there are postsynaptic D2 receptors present on VTA GABAergic neurons (Steffensen et al., 2008). The *Drd2* shRNAs used in this study are driven by a non-selective U6 promoter; thus presumably putative *Drd2* in VTA GABAergic neurons was also knocked down, and this assumption is supported by the GFP signal evident in non-dopaminergic neurons in Figure 1. Pharmacological activation of D2 receptors has been shown to increase the firing rates of VTA GABAergic neurons (Ludlow et al., 2009; Steffensen et al., 2008; but see Margolis et al., 2012). Since GABAergic interneurons in the VTA provide local inhibitory inputs onto dopamine cells (Omelchenko and Sesack, 2009; Tan et al., 2012; van Zessen et al., 2012), knockdown of D2 receptors in GABAergic cells would presumably result in a decrease in inhibitory tone, adding to the reduction in autoinhibition due to the knockdown of autoreceptors in dopamine neurons. In addition, VTA GABAergic projection neurons target the nucleus accumbens and prefrontal cortex (Carr and Sesack, 2000; Van Bockstaele and Pickel, 1995), and projections to such brain regions as the lateral hypothalamus, mediodorsal thalamus, central amygdala, periaqueductal gray, and the lateral habenula have also been demonstrated in the rodent brain (Breton et al., 2019; Root et al., 2014; Zhou et al., 2019). Knockdown of D2 receptors on GABAergic

neurons, then, certainly may contribute, in part, to both the magnitude and anatomical extent of the effects described in this study.

There are likely many other factors that could contribute to the widespread effects of alterations in the regulation of dopamine in the VTA that occur as a result of the knockdown. For example, dopamine D1 receptors are located on GABAergic and glutamatergic afferents to the VTA. Activation of these receptors can alter the firing patterns of these afferents (Cameron and Williams, 1993, 1995; Kalivas and Duffy, 1995). Knockdown-induced changes in dopamine tone in the VTA could therefore alter the activity of these neurons and in turn the circuits of which they are a part. While it is beyond the scope of this investigation to isolate and identify the specific downstream mechanisms which result in the observed effects of D2 knockdown in the VTA, these findings highlight the importance of the VTA's influence beyond the nucleus accumbens.

Studies using mutant mouse models to investigate D2 autoreceptor function initially used D2-deficient mice which lacked both presynaptic and postsynaptic D2 receptor populations throughout the brain (Baik et al., 1995; Benoit-Marand et al., 2001, 2011; Dickinson et al., 1999; Jung et al., 1999; L'Hirondel et al., 1998; Mercuri et al., 1997; Schmitz et al., 2002). Complete ablation of D2 receptors, however, resulted in mice with dyskinesias and abnormal growth patterns (Baik et al., 1995; Kelly et al., 1998). More recently, conditional mutant mice were generated in which D2 autoreceptors were selectively knocked out, thus sparing post-synaptic D2 heteroreceptors (Anzalone et al., 2012; Bello et al., 2011; Holroyd et al., 2015). These studies have demonstrated increases in locomotor activity and sensitivity to cocaine, as well as sensitivity to drug-paired cues following ablation of D2 autoreceptors (Bello et al., 2011; Holroyd et al., 2015). Mice lacking D2 autoreceptors have also been shown to exhibit deficiencies in both acquisition of the learning criterion in a spatial reversal learning task, as well as the ability to maintain a prolonged nose-poke, indicating diminished response inhibition (Linden et al., 2018).

The viral knockdown approach used in the current study, however, provides a targeted, partial rather than complete, reduction in VTA D2 receptors, thus resulting in a model that more closely recapitulates the conditions in human studies in which a high degree of variability has been observed in midbrain D2 receptor levels (Buckholtz et al., 2010; Zald et al., 2008, 2010). Using an identical procedure to the current study, an association between reductions in the levels of D2 receptor mRNA in the VTA and increased cocaine intake was demonstrated in rodents using a fixed ratio schedule of reinforcement (Chen et al., 2018). Employing a similar procedure, Bernosky-Smith and colleagues (2018) used an adeno-associated viral vector in rats to determine that D2 knockdown in the VTA resulted in more impulsive choices as measured by a delay-discounting task. The reduced *Drd2* mRNA levels in the VTA likely increased dopamine neuron excitability and terminal dopamine release. The functional alterations observed in the current study may underlie the spectrum of behavioral effects observed in animals deficient in midbrain D2 receptors.

In the present study we chose to use lentivirus, rather than adeno-associated virus (AAV), to knock down *Drd2* in the VTA because of the restricted passive diffusion of lentivirus in the brain. Lentiviral particles are about 100 nm in diameter, whereas AAV is around 20-30 nm

(Artimo et al., 2012). The extracellular space in the rat brain is estimated to be 30-60 nm (Thorne and Nicholson, 2006); therefore, the large size of lentivirus hinders its diffusion through the parenchyma of the brain. It has been reported that injections of various volumes of lentivirus into the rat cortex or hippocampus produce an infection within a spherical region of about 400-600 μm in diameter (Osten et al., 2006). Although lentiviral transduction is limited in its spatial extent, the lentivirus encoding GFP and Drd2 shRNA is randomly integrated into the rat genome; thus, the reporter protein (GFP) is synthesized by cells and transported to different cellular compartments, which may project beyond the site of the injection. Likewise, the synthesis of D2 receptor proteins is reduced not only in the VTA, but also in projection sites originating from VTA cell bodies.

In humans, dopamine D_2-like receptors in the midbrain have been measured with the radioligand [^{18}F]fallypride and positron emission tomography (Buckholtz et al., 2010; Dang et al., 2018; Zald et al., 2008, 2010). These studies in healthy volunteers showed that there is a wide range of individual differences in D_2-like receptor availability within the midbrain and that these levels were inversely correlated with measures of novelty seeking (Zald et al., 2008). This is consistent with rodent studies in which high novelty-responding rats exhibited greater levels of basal activity of dopamine neurons and reduced sensitivity of midbrain autoreceptors as compared to those rats that exhibited lower locomotor responses to novelty (Marinelli and White, 2000). Midbrain D2 receptor availability in healthy volunteers was also found to negatively correlate with scores on the Barratt's Impulsiveness Scale (BIS-11), suggesting that these individuals with low availability express higher levels of trait impulsivity (Buckholtz et al., 2010) than those with higher levels of midbrain D2 receptor availability. These investigators also showed that the impulsivity scores were positively correlated with amphetamine-induced dopamine release in the striatum of these same subjects. These data demonstrate that the normal variability in D2 receptor regulation of midbrain dopamine neurons and the consequent differences in dopamine release in the striatum can have significant behavioral consequences. The knockdown approach used in the current study results in a reduction of approximately 30% in midbrain autoreceptor *Drd2* mRNA, rather than a complete elimination as in genetic knockouts, and more closely mimics the individual differences observed in these studies of healthy subjects. These data, along with those of the present study, clearly show that even relatively small perturbations in dopamine regulation can have large effects on behavior, as well as widespread consequences for functional activity throughout the brain.

In summary, the results of the present study demonstrate that partial reduction of D2 receptors in the VTA results in widespread alterations in functional activity throughout the brain in both direct terminal fields of the VTA such as the ventral striatum, as well as many areas in which dopamine projections are far less dense, such as the cerebellum, or are only indirectly innervated by the VTA, such as the globus pallidus. These findings suggest that even relatively small changes in dopamine regulation can have profound effects in many systems within the brain, including sensory, cognitive, motor and emotional networks, thus potentially influencing a wide range of behaviors.

4. Experimental Procedure

4.1 Animals

Adult male Sprague-Dawley rats weighing 325-350g (Envigo, Indianapolis, IN) were housed in a temperature and humidity controlled vivarium on a 12-hour reversed light cycle (lights on at 18:00 hours). Upon arrival, animals were single-housed and food and water were available *ad libitum*. All procedures were conducted during the dark phase of the light/dark cycle. Animals were randomly assigned to one of three groups: *Drd2*KD, SCR, and PBS. The experimenter was blind to group assignment. All procedures were performed in accordance with the National Institutes of Health *Guide for the Care and Use of Laboratory Animals* and were approved by the Animal Care and Use Committee of Wake Forest School of Medicine.

4.2 Rat dopamine D2 receptor shRNA-containing lentiviral vectors

The *Drd2* mRNA levels were knocked down in the VTA via microinjection of lentivirus encoding *Drd2* shRNAs and the gene encoding GFP as previously described (Chen et al., 2018). Briefly, four siRNA sequences against the rat D2 receptors (accession number: NM_012547.1) were selected using the Dharmacon siDESIGN siRNA design tool (Horizon, Cambridge, UK). Sequences targeting both the long and short forms of the rat D2 receptors were: a) ccaccaactacttgatagtca, b) catcgtcactctgctggtcta, c) cttcggactcaacaatacaga, and d) caacctgaagacaccactcaa. *Drd2* shRNAs were inserted into psi-LVRU6GP (GeneCopoeia, Rockville, MD) to engineer psi-U6-*Drd2*shRNA-SV40-eGFP-IRES-Puro, in which *Drd2* shRNA was driven by human U6 promoters and the SV40 promoter drives both eGFP and a puromycin resistance gene using an internal ribosome entry site (IRES). The scrambled siRNA sequence (gcctatcaccgtcataata) does not correspond to any known rat sequence.

Lentivirus was produced in HEK 293 cells as described previously using the 3rd generation packaging system followed by purification and concentration (Chen et al., 2018). The titer of the lentivirus was 2.5 x 10^{8} TU/ml, as determined by a p24 ELISA kit (Sigma Aldrich, St Louis, MO). Control lentivirus was generated in the same way from the lentiviral vector containing the scrambled shRNA.

4.3 Surgical procedures

Animals were anesthetized with isoflurane (2.5-3%), administered a prophylactic dose of ketoprofen (3.0 mg/kg; s.c.) and closely monitored throughout the procedure. Rats were fitted into a stereotaxic apparatus (Stoelting, Wood Dale, IL), the scalp was shaved and cleaned, and an incision was made along the midline of the skull. The skin and muscle layers were retracted and bilateral holes were drilled into the skull at coordinates above the VTA (AP −5.7mm from Bregma, lateral ±0.7mm). A 10 μl Hamilton syringe was used to infuse 1μl of PBS or virus at a depth of −7.7mm from top of brain. Stereotaxic coordinates were taken from Paxinos and Watson (1998). Lentiviral infusions were delivered at a rate of 0.25μl/minute. Control animals were injected with phosphate buffered saline (PBS group) or with lentivirus expressing scrambled shRNA (SCR group). The needle was kept in place for five minutes after each injection to allow time for diffusion, then gradually retracted over a period of two minutes to minimize backflow of virus along the needle track. The drill holes

were sealed with bone wax and the scalp incision was closed with absorbable sutures. Animals were closely monitored and administered ketoprofen (3.0 mg/kg; s.c.) at 24, 48, and 72 hours post-surgery.

Femoral catheterizations for the 2-DG experiments were carried out 24 hours prior to the procedure to allow for recovery and anesthetic clearance. Animals were anesthetized with isoflurane (2-3%), the surgical sites were shaved and cleaned, and a prophylactic dose of ketoprofen (3.0 mg/kg, s.c.) was administered. An incision was made in the left inguinal region and the femoral bundle was isolated. Catheters were filled with heparinized saline, inserted into the femoral artery and vein and secured, and then subcutaneously tunneled to a point on the back where they exited between the scapulae. Catheters were coiled and secured with a rodent harness (Instech, Plymouth Meeting, PA). Animals were monitored closely for recovery from anesthesia, and were returned to their home cages until the 2-DG procedure.

4.4 2-[^{14}C]deoxyglucose procedure

Local cerebral glucose utilization was measured according to the method of Sokoloff and colleagues (Sokoloff et al., 1977), as adapted for use in the freely moving rat (Crane and Porrino, 1989). The procedure was performed 21 days after viral infusions when maximal lentiviral knockdown is attained (Chen et al., 2018). Rats (in their home cages) were allowed to acclimate to the experimental room for 15 minutes prior to initiation of the procedure. Rats were administered an intravenous pulse of 2-DG (75 μCi/kg; specific activity 50-55 mCi/mmol; PerkinElmer, Waltham, MA), followed by a flush of 0.2 ml heparinized saline. Timed arterial blood samples were taken over a period of 45 minutes using a schedule designed to capture peak blood 2-DG levels. The arterial catheter was flushed with heparinized saline between samples in order to maintain patency. Samples were immediately centrifuged and plasma concentrations of 2-DG and glucose were assessed. At the end of the 45 minute sampling procedure animals were euthanized with an intravenous bolus of 0.3 ml Fatal Plus (pentobarbital sodium 390 mg/ml; Patterson Veterinary, Greeley, CO). Brains were rapidly removed, frozen in isopentane at −45°C, and then stored at −80°C until sectioning for autoradiography.

Brains were sectioned (20 μm; coronal sections) in a cryostat maintained at −20°C. Four of every 10 sections were collected onto glass coverslips, and quick-dried on a hotplate at 60°C for 2-DG autoradiography. In addition six of every 10 sections through the midbrain were thaw-mounted onto Adhesion-Plus microscope slides (Brain Research Labs, Waban, MA) for immunofluorescence verification of lentiviral infection sites. Slides were dessicated and stored at −80°C until processing. Sections for autoradiography were apposed to film (Min-R 2000; Carestream Health, Rochester, NY) alongside calibrated [^{14}C] standards (Amersham, Arlington Heights, IL) for 12 to 15 days. Autoradiograms were analyzed by quantitative densitometry with a computerized image processing system (MCID, Imaging Research, Linton, UK). Optical density measurements for each brain structure were made in a minimum of five sections. LCGU was calculated using the operation equation defined by Sokoloff et al. (1977). Rates of glucose utilization were determined in 34 brain structures; structures were identified according to the rat brain atlas of Paxinos and Watson (1998).

4.5 Immunofluorescence staining of tissue sections

In order to confirm that lentiviral particles were taken up by dopamine cells in the VTA, immunofluorescent intensities of TH and GFP were imaged in fresh-frozen tissue sections collected when brains were sectioned for 2-DG autoradiography. Sections were post-fixed for 1.5 hours at 4°C, then washed in PBS. Sections were blocked in 10% normal donkey serum (NDS) containing 0.3% Triton-X, then incubated in primary antibody solution overnight at 4°C, washed in PBS, and incubated in secondary antibody solution for one hour at room temperature. The primary antibody solution contained rabbit anti-TH antibody (1:1000; #AB152, EMD Millipore, Temecula, CA), chicken anti-GFP antibody (1:500; #GFP-1020, Aves Labs, Tigard, OR), 10% NDS, and 0.1% Triton-X in PBS. The secondary antibody solution contained Alexa Fluor®594-conjugated donkey anti-rabbit antibody (1:500; #ab150076, Abcam, Cambridge, MA), Alexa Fluor®488-donkey anti-chicken antibody (1:500; #703-545-155, Jackson ImmunoResearch, West Grove, PA), and 10% NDS in PBS. Slides were washed in PBS, and coverslipped using ProLong Gold anti-fade reagent (Fisher Scientific, Hampton, NH) for imaging. Images of fluorescent signals were acquired with a Zeiss LSM 710 laser scanning confocal microscope. Alexa 488 and 594 were excited with Argon and HeNe lasers, respectively. Animals in which injections were misplaced were excluded from the analysis.

4.6 Statistical Analysis

Standard statistics software (SPSS, Chicago, IL) was used for statistical analysis. Global rates of glucose utilization were calculated as the weighted average of rates of glucose metabolism across analyzed brain regions. Rates of glucose utilization were analyzed in specific functional groups of brain regions (mesolimbic, nigrostriatal, limbic, cortex and thalamus, and brainstem). Rates from the two control groups (PBS and SCR) were combined, as no significant statistical differences between the two groups were observed in any brain region; however data values from these two groups, along with the *Drd2*KD group are shown individually in Table 1. Statistical analysis was accomplished using a two-way ANOVA, brain region group X treatment (PBS vs SCR vs *Drd2*KD) with brain region group as a repeated measure. These were followed by planned Bonferroni's tests for multiple comparisons. Statistical significance was considered as $p < 0.05$.

Acknowledgements

This work was supported by National Institute of Drug Abuse grant numbers P50DA006634 and R01DA042862. Deborah Luessen was supported by NIH T32AA007565.

References

Aghajanian GK, Bunney BS (1977) Dopamine"autoreceptors": pharmacological characterization by microiontophoretic single cell recording studies. Naunyn Schmiedebergs Arch Pharmacol 297:1–7. [PubMed: 193046]

Anden N-E, Dahlstrom A, Fuxe K, Larsson L, Olson U, Ungerstedt U (1966) Ascending monoamine neurons to the telencephalon and diencephalon. Acta Physiologica Scandinavica 67:313–326. DOI: 10.1111/j.1748-1716.1966.tb03318.x

Anzalone A, Lizardi-Ortiz JE, Ramos M, De Mei C, Hopf FW, Iaccarino C, Halbout B, Jacobsen J, Kinoshita C, Welter M, Caron MG, Bonci A, Sulzer D, Borrelli E (2012) Dual control of dopamine

synthesis and release by presynaptic and postsynaptic dopamine D2 receptors. J Neurosci 32:9023–9034. DOI: 10.1523/JNEUROSCI.0918-12.2012 [PubMed: 22745501]

Artimo P, Jonnalagedda M, Arnold K, Baratin D, Csardi G, de Castro E, Duvaud S, Flegel V, Fortier A, Gasteiger E, Grosdidier A, Hernandez C, Ioannidis V, Kuznetsov D, Liechti R, Moretti S, Mostaguir K, Redaschi N, Rossier G, Xenarios I, Stockinger H (2012) ExPASy: SIB bioinformatics resource portal. Nucleic Acids Res 40:W597–603. DOI: 10.1093/nar/gks400 [PubMed: 22661580]

Baik JH, Picetti R, Saiardi A, Thiriet G, Dierich A, Depaulis A, Le Meur M, Borrelli E (1995) Parkinsonian-like locomotor impairment in mice lacking dopamine D2 receptors. Nature 377:424–428. DOI: 10.1038/377424a0 [PubMed: 7566118]

Beaulieu JM, Gainetdinov RR (2011) The physiology, signaling, and pharmacology of dopamine receptors. Pharmacol Rev 63:182–217. DOI: 10.1124/pr.110.002642 [PubMed: 21303898]

Beckstead MJ, Grandy DK, Wickman K, Williams JT (2004) Vesicular dopamine release elicits an inhibitory postsynaptic current in midbrain dopamine neurons. Neuron 42:939–946. DOI: 10.1016/j.neuron.2004.05.019 [PubMed: 15207238]

Beckstead RM, Domesick VB, Nauta WJ (1979) Efferent connections of the substantia nigra and ventral tegmental area in the rat. Brain Res 175:191–217. DOI: 10.1016/0006-8993(79)91001-1 [PubMed: 314832]

Bello EP, Mateo Y, Gelman DM, Noain D, Shin JH, Low MJ, Alvarez VA, Lovinger DM, Rubinstein M (2011) Cocaine supersensitivity and enhanced motivation for reward in mice lacking dopamine D2 autoreceptors. Nat Neurosci 14:1033–1038. DOI: 10.1038/nn.2862 [PubMed: 21743470]

Benoit-Marand M, Ballion B, Borrelli E, Boraud T, Gonon F (2011) Inhibition of dopamine uptake by D2 antagonists: an in vivo study. J Neurochem 116:449–458. DOI: 10.1111/j.1471-4159.2010.07125.x [PubMed: 21128941]

Benoit-Marand M, Borrelli E, Gonon F (2001) Inhibition of dopamine release via presynaptic D2 receptors: time course and functional characteristics in vivo. J Neurosci 21:9134–9141. [PubMed: 11717346]

Bernosky-Smith KA, Qiu YY, Feja M, Lee YB, Loughlin B, Li JX, Bass CE (2018) Ventral tegmental area D2 receptor knockdown enhances choice impulsivity in a delay-discounting task in rats. Behav Brain Res 341:129–134. DOI: 10.1016/j.bbr.2017.12.029 [PubMed: 29287910]

Breton JM, Charbit AR, Snyder BJ, Fong PTK, Dias EV, Himmels P, Lock H, Margolis EB (2019) Relative contributions and mapping of ventral tegmental area dopamine and GABA neurons by projection target in the rat. J Comp Neurol 527:916–941. DOI: 10.1002/cne.24572 [PubMed: 30393861]

Buckholtz JW, Treadway MT, Cowan RL, Woodward ND, Li R, Ansari MS, Baldwin RM, Schwartzman AN, Shelby ES, Smith CE, Kessler RM, Zald DH (2010) Dopaminergic network differences in human impulsivity. Science 329:532 DOI: 10.1126/science.1185778 [PubMed: 20671181]

Cameron DL, Williams JT (1993) Dopamine D1 receptors facilitate transmitter release. Nature 366:344–347. DOI: 10.1038/366344a0 [PubMed: 8247128]

Cameron DL, Williams JT (1995) Opposing roles for dopamine and serotonin at presynaptic receptors in the ventral tegmental area. Clin Exp Pharmacol Physiol 22:841–845. [PubMed: 8593741]

Carr DB, Sesack SR (2000) GABA-containing neurons in the rat ventral tegmental area project to the prefrontal cortex. Synapse 38:114–123. DOI: 10.1002/1098-2396(200011)38:2<114::AID-SYN2>3.0.CO;2-R [PubMed: 11018785]

Chen R, McIntosh S, Hemby SE, Sun H, Sexton T, Martin TJ, Childers SR (2018) High and low doses of cocaine intake are differentially regulated by dopamine D2 receptors in the ventral tegmental area and the nucleus accumbens. Neurosci Lett 671:133–139. DOI: 10.1016/j.neulet.2018.02.026 [PubMed: 29454035]

Courtney NA, Mamaligas AA, Ford CP (2012) Species differences in somatodendritic dopamine transmission determine D2-autoreceptor-mediated inhibition of ventral tegmental area neuron firing. J Neurosci 32:13520–13528. DOI: 10.1523/JNEUROSCI.2745-12.2012 [PubMed: 23015441]

Crane AM, Porrino LJ (1989) Adaptation of the quantitative 2-[14C]deoxyglucose method for use in freely moving rats. Brain Res 499:87–92. [PubMed: 2804673]

Dang LC, Samanez-Larkin GR, Castrellon JJ, Perkins SF, Cowan RL, Zald DH (2018) Individual differences in dopamine D2 receptor availability correlate with reward valuation. Cogn Affect Behav Neurosci 18:739–747. DOI: 10.3758/s13415-018-0601-9 [PubMed: 29725947]

de Jong JW, Roelofs TJ, Mol FM, Hillen AE, Meijboom KE, Luijendijk MC, van der Eerden HA, Garner KM, Vanderschuren LJ, Adan RA (2015) Reducing Ventral Tegmental Dopamine D2 Receptor Expression Selectively Boosts Incentive Motivation. Neuropsychopharmacology 40:2085–2095. DOI: 10.1038/npp.2015.60 [PubMed: 25735756]

Decot HK, Namboodiri VM, Gao W, McHenry JA, Jennings JH, Lee SH, Kantak PA, Jill Kao YC, Das M, Witten IB, Deisseroth K, Shih YI, Stuber GD (2017) Coordination of Brain-Wide Activity Dynamics by Dopaminergic Neurons. Neuropsychopharmacology 42:615–627. DOI: 10.1038/npp.2016.151 [PubMed: 27515791]

Dickinson SD, Sabeti J, Larson GA, Giardina K, Rubinstein M, Kelly MA, Grandy DK, Low MJ, Gerhardt GA, Zahniser NR (1999) Dopamine D2 receptor-deficient mice exhibit decreased dopamine transporter function but no changes in dopamine release in dorsal striatum. J Neurochem 72:148–156. [PubMed: 9886065]

Fallon JH, Moore RY (1978) Catecholamine innervation of the basal forebrain. IV. Topography of the dopamine projection to the basal forebrain and neostriatum. J Comp Neurol 180:545–580. DOI: 10.1002/cne.901800310 [PubMed: 659674]

Ford CP (2014) The role of D2-autoreceptors in regulating dopamine neuron activity and transmission. Neuroscience 282:13–22. DOI: 10.1016/j.neuroscience.2014.01.025 [PubMed: 24463000]

Gantz SC, Bunzow JR, Williams JT (2013) Spontaneous inhibitory synaptic currents mediated by a G protein-coupled receptor. Neuron 78:807–812. DOI: 10.1016/j.neuron.2013.04.013 [PubMed: 23764286]

Gasbarri A, Packard MG, Campana E, Pacitti C (1994a) Anterograde and retrograde tracing of projections from the ventral tegmental area to the hippocampal formation in the rat. Brain Res Bull 33:445–452. DOI: 10.1016/0361-9230(94)90288-7 [PubMed: 8124582]

Gasbarri A, Verney C, Innocenzi R, Campana E, Pacitti C (1994b) Mesolimbic dopaminergic neurons innervating the hippocampal formation in the rat: a combined retrograde tracing and immunohistochemical study. Brain Res 668:71–79. DOI: 10.1016/0006-8993(94)90512-6 [PubMed: 7704620]

Grace AA (2016) Dysregulation of the dopamine system in the pathophysiology of schizophrenia and depression. Nat Rev Neurosci 17:524–532. DOI: 10.1038/nrn.2016.57 [PubMed: 27256556]

Hikosaka O, Bromberg-Martin E, Hong S, Matsumoto M (2008) New insights on the subcortical representation of reward. Curr Opin Neurobiol 18:203–208. DOI: 10.1016/j.conb.2008.07.002 [PubMed: 18674617]

Holroyd KB, Adrover MF, Fuino RL, Bock R, Kaplan AR, Gremel CM, Rubinstein M, Alvarez VA (2015) Loss of feedback inhibition via D2 autoreceptors enhances acquisition of cocaine taking and reactivity to drug-paired cues. Neuropsychopharmacology 40:1495–1509. DOI: 10.1038/npp.2014.336 [PubMed: 25547712]

Ikai Y, Takada M, Shinonaga Y, Mizuno N (1992) Dopaminergic and non-dopaminergic neurons in the ventral tegmental area of the rat project, respectively, to the cerebellar cortex and deep cerebellar nuclei. Neuroscience 51:719–728. DOI: 10.1016/0306-4522(92)90310-x [PubMed: 1362601]

Jung MY, Skryabin BV, Arai M, Abbondanzo S, Fu D, Brosius J, Robakis NK, Polites HG, Pintar JE, Schmauss C (1999) Potentiation of the D2 mutant motor phenotype in mice lacking dopamine D2 and D3 receptors. Neuroscience 91:911–924. [PubMed: 10391470]

Kalivas PW, Duffy P (1995) D1 receptors modulate glutamate transmission in the ventral tegmental area. J Neurosci 15:5379–5388. [PubMed: 7623160]

Kelly MA, Rubinstein M, Phillips TJ, Lessov CN, Burkhart-Kasch S, Zhang G, Bunzow JR, Fang Y, Gerhardt GA, Grandy DK, Low MJ (1998) Locomotor activity in D2 dopamine receptor-deficient mice is determined by gene dosage, genetic background, and developmental adaptations. J Neurosci 18:3470–3479. [PubMed: 9547254]

Klitenick MA, Deutch AY, Churchill L, Kalivas PW (1992) Topography and functional role of dopaminergic projections from the ventral mesencephalic tegmentum to the ventral pallidum. Neuroscience 50:371–386. DOI: 10.1016/0306-4522(92)90430-a [PubMed: 1279461]

Koob GF (1996) Hedonic valence, dopamine and motivation. Mol Psychiatry 1:186–189. [PubMed: 9118342]

Koob GF, Volkow ND (2010) Neurocircuitry of addiction. Neuropsychopharmacology 35:217–238. DOI: 10.1038/npp.2009.110 [PubMed: 19710631]

L'Hirondel M, Cheramy A, Godeheu G, Artaud F, Saiardi A, Borrelli E, Glowinski J (1998) Lack of autoreceptor-mediated inhibitory control of dopamine release in striatal synaptosomes of D2 receptor-deficient mice. Brain Res 792:253–262. [PubMed: 9593923]

Lacey MG, Mercuri NB, North RA (1987) Dopamine acts on D2 receptors to increase potassium conductance in neurones of the rat substantia nigra zona compacta. J Physiol 392:397–416. DOI: 10.1113/jphysiol.1987.sp016787 [PubMed: 2451725]

Linden J, James AS, McDaniel C, Jentsch JD (2018) Dopamine D2 Receptors in Dopaminergic Neurons Modulate Performance in a Reversal Learning Task in Mice. eNeuro 5 DOI: 10.1523/ENEURO.0229-17.2018

Lindvall O, Bjorklund A (1974) The organization of the ascending catecholamine neuron systems in the rat brain as revealed by the glyoxylic acid fluorescence method. Acta Physiol Scand Suppl 412:1–48. [PubMed: 4531814]

Lohani S, Poplawsky AJ, Kim SG, Moghaddam B (2017) Unexpected global impact of VTA dopamine neuron activation as measured by opto-fMRI. Mol Psychiatry 22:585–594. DOI: 10.1038/mp.2016.102 [PubMed: 27457809]

Ludlow KH, Bradley KD, Allison DW, Taylor SR, Yorgason JT, Hansen DM, Walton CH, Sudweeks SN, Steffensen SC (2009) Acute and chronic ethanol modulate dopamine D2-subtype receptor responses in ventral tegmental area GABA neurons. Alcohol Clin Exp Res 33:804–811. DOI: 10.1111/j.1530-0277.2009.00899.x [PubMed: 19298327]

Margolis EB, Toy B, Himmels P, Morales M, Fields HL (2012) Identification of rat ventral tegmental area GABAergic neurons. PLoS One 7:e42365 DOI: 10.1371/journal.pone.0042365 [PubMed: 22860119]

Marinelli M, White FJ (2000) Enhanced vulnerability to cocaine self-administration is associated with elevated impulse activity of midbrain dopamine neurons. J Neurosci 20:8876–8885. [PubMed: 11102497]

Mercuri NB, Saiardi A, Bonci A, Picetti R, Calabresi P, Bernardi G, Borrelli E (1997) Loss of autoreceptor function in dopaminergic neurons from dopamine D2 receptor deficient mice. Neuroscience 79:323–327. [PubMed: 9200717]

Morales M, Margolis EB (2017) Ventral tegmental area: cellular heterogeneity, connectivity and behaviour. Nat Rev Neurosci 18:73–85. DOI: 10.1038/nrn.2016.165 [PubMed: 28053327]

Nestler EJ, Carlezon WA, Jr. (2006) The mesolimbic dopamine reward circuit in depression. Biol Psychiatry 59:1151–1159. DOI: 10.1016/j.biopsych.2005.09.018 [PubMed: 16566899]

Nutt DJ, Lingford-Hughes A, Erritzoe D, Stokes PR (2015) The dopamine theory of addiction: 40 years of highs and lows. Nat Rev Neurosci 16:305–312. DOI: 10.1038/nrn3939 [PubMed: 25873042]

Omelchenko N, Sesack SR (2009) Ultrastructural analysis of local collaterals of rat ventral tegmental area neurons: GABA phenotype and synapses onto dopamine and GABA cells. Synapse 63:895–906. DOI: 10.1002/syn.20668 [PubMed: 19582784]

Osten P, Dittgen T, Licznerski P (2006) Lentivirus-Based Genetic Manipulations in Neurons In Vivo In: The Dynamic Synapse: Molecular Methods in Ionotropic Receptor Biology(Kittler JT and Moss SJ, eds) Boca Raton (FL).

Paxinos G, Watson C (1998) The rat brain in stereotaxic coordinates. San Diego: Academic Press.

Pillai G, Brown NA, McAllister G, Milligan G, Seabrook GR (1998) Human D2 and D4 dopamine receptors couple through betagamma G-protein subunits to inwardly rectifying K+ channels (GIRK1) in a Xenopus oocyte expression system: selective antagonism by L-741,626 and L-745,870 respectively. Neuropharmacology 37:983–987. DOI: 10.1016/s0028-3908(98)00092-6 [PubMed: 9833627]

Pucak ML, Grace AA (1994) Evidence that systemically administered dopamine antagonists activate dopamine neuron firing primarily by blockade of somatodendritic autoreceptors. J Pharmacol Exp Ther 271:1181–1192. [PubMed: 7996424]

Robbins TW (2003) Dopamine and cognition. Curr Opin Neurol 16 Suppl 2:S1–2. DOI: 10.1097/00019052-200312002-00001 [PubMed: 15129843]

Root DH, Mejias-Aponte CA, Zhang S, Wang HL, Hoffman AF, Lupica CR, Morales M (2014) Single rodent mesohabenular axons release glutamate and GABA. Nat Neurosci 17:1543–1551. DOI: 10.1038/nn.3823 [PubMed: 25242304]

Salamone JD, Correa M (2012) The mysterious motivational functions of mesolimbic dopamine. Neuron 76:470–485. DOI: 10.1016/j.neuron.2012.10.021 [PubMed: 23141060]

Schmitz Y, Schmauss C, Sulzer D (2002) Altered dopamine release and uptake kinetics in mice lacking D2 receptors. J Neurosci 22:8002–8009. [PubMed: 12223553]

Schultz W (2015) Neuronal Reward and Decision Signals: From Theories to Data. Physiol Rev 95:853–951. DOI: 10.1152/physrev.00023.2014 [PubMed: 26109341]

Sesack SR, Aoki C, Pickel VM (1994) Ultrastructural localization of D2 receptor-like immunoreactivity in midbrain dopamine neurons and their striatal targets. J Neurosci 14:88–106. [PubMed: 7904306]

Sokoloff L, Reivich M, Kennedy C, Des Rosiers MH, Patlak CS, Pettigrew KD, Sakurada O, Shinohara M (1977) The [14C]deoxyglucose method for the measurement of local cerebral glucose utilization: theory, procedure, and normal values in the conscious and anesthetized albino rat. J Neurochem 28:897–916. [PubMed: 864466]

Steffensen SC, Taylor SR, Horton ML, Barber EN, Lyle LT, Stobbs SH, Allison DW (2008) Cocaine disinhibits dopamine neurons in the ventral tegmental area via use-dependent blockade of GABA neuron voltage-sensitive sodium channels. Eur J Neurosci 28:2028–2040. DOI: 10.1111/j.1460-9568.2008.06479.x [PubMed: 19046384]

Swanson LW (1982) The projections of the ventral tegmental area and adjacent regions: a combined fluorescent retrograde tracer and immunofluorescence study in the rat. Brain Res Bull 9:321–353. DOI: 10.1016/0361-9230(82)90145-9 [PubMed: 6816390]

Tan KR, Yvon C, Turiault M, Mirzabekov JJ, Doehner J, Labouebe G, Deisseroth K, Tye KM, Luscher C (2012) GABA neurons of the VTA drive conditioned place aversion. Neuron 73:1173–1183. DOI: 10.1016/j.neuron.2012.02.015 [PubMed: 22445344]

Thierry AM, Blanc G, Sobel A, Stinus L, Glowinski J (1973) Dopaminergic terminals in the rat cortex. Science 182:499–501. DOI: 10.1126/science.182.4111.499 [PubMed: 4744179]

Thorne RG, Nicholson C (2006) In vivo diffusion analysis with quantum dots and dextrans predicts the width of brain extracellular space. Proc Natl Acad Sci U S A 103:5567–5572. DOI: 10.1073/pnas.0509425103 [PubMed: 16567637]

Van Bockstaele EJ, Pickel VM (1995) GABA-containing neurons in the ventral tegmental area project to the nucleus accumbens in rat brain. Brain Res 682:215–221. DOI: 10.1016/0006-8993(95)00334-m [PubMed: 7552315]

van Zessen R, Phillips JL, Budygin EA, Stuber GD (2012) Activation of VTA GABA neurons disrupts reward consumption. Neuron 73:1184–1194. DOI: 10.1016/j.neuron.2012.02.016 [PubMed: 22445345]

White FJ, Wang RY (1984) A10 dopamine neurons: role of autoreceptors in determining firing rate and sensitivity to dopamine agonists. Life Sci 34:1161–1170. [PubMed: 6708722]

Zald DH, Cowan RL, Riccardi P, Baldwin RM, Ansari MS, Li R, Shelby ES, Smith CE, McHugo M, Kessler RM (2008) Midbrain dopamine receptor availability is inversely associated with novelty-seeking traits in humans. J Neurosci 28:14372–14378. DOI: 10.1523/JNEUROSCI.2423-08.2008 [PubMed: 19118170]

Zald DH, Woodward ND, Cowan RL, Riccardi P, Ansari MS, Baldwin RM, Smith CE, Hakyemez H, Li R, Kessler RM (2010) The interrelationship of dopamine D2-like receptor availability in striatal and extrastriatal brain regions in healthy humans: a principal component analysis of [18F]fallypride binding. Neuroimage 51:53–62. DOI: 10.1016/j.neuroimage.2010.02.006 [PubMed: 20149883]

Zhou Z, Liu X, Chen S, Zhang Z, Liu Y, Montardy Q, Tang Y, Wei P, Liu N, Li L, Song R, Lai J, He X, Chen C, Bi G, Feng G, Xu F, Wang L (2019) A VTA GABAergic Neural Circuit Mediates Visually Evoked Innate Defensive Responses. Neuron 103:473–488 e476 DOI: 10.1016/j.neuron.2019.05.027 [PubMed: 31202540]

Highlights

- Viral knockdown of VTA D2 receptors alters local cerebral glucose metabolism
- Elevations in glucose metabolism were seen in the terminal fields of the mesocorticolimbic system
- Knockdowns also had wide-ranging effects throughout other brain systems

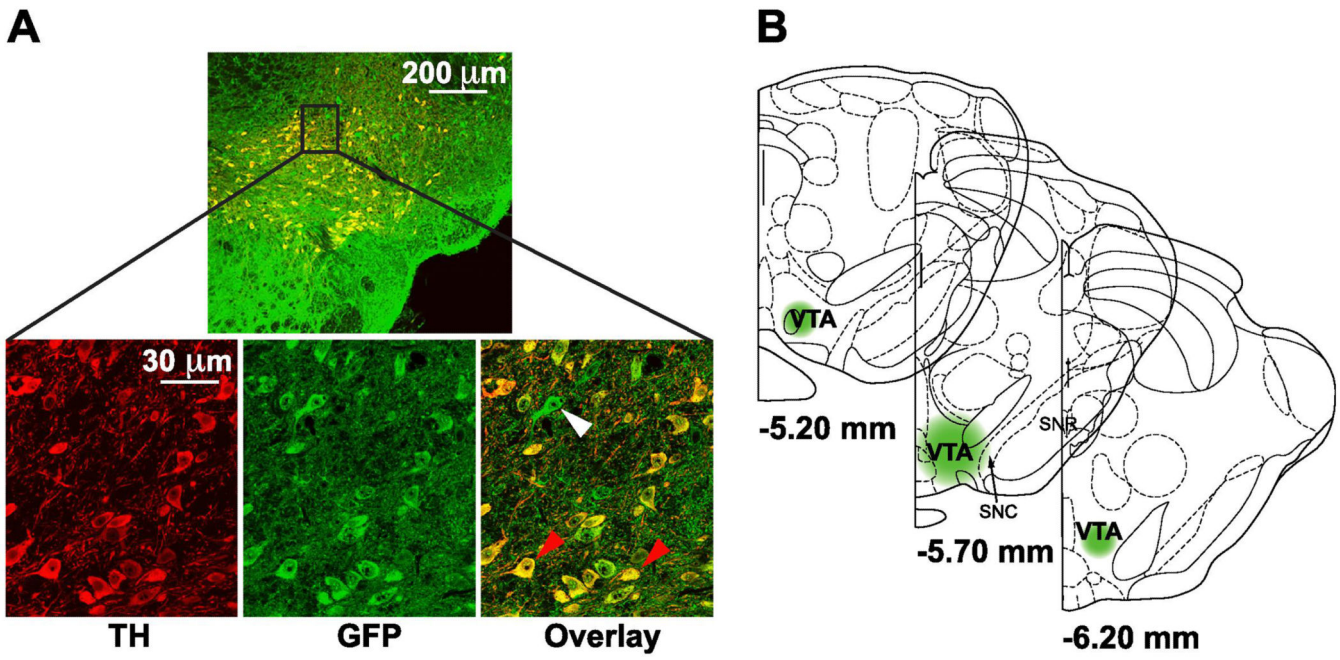

Figure 1.

A. Representative images of immunofluorescence staining for TH (red), GFP (green), and an overlay (yellow) of both markers in the VTA of a rat infected with lentivirus. Red arrows in the overlay image indicate putative dopamine cells double-labeled for TH and GFP. White arrow indicates a virally-infected non-dopaminergic cell. B. Schematic of rat brain sections at the level of the VTA showing the approximate extent of viral transduction. SNC, substantia nigra compacta; SNR, substantia nigra reticulata; VTA, ventral tegmental area.

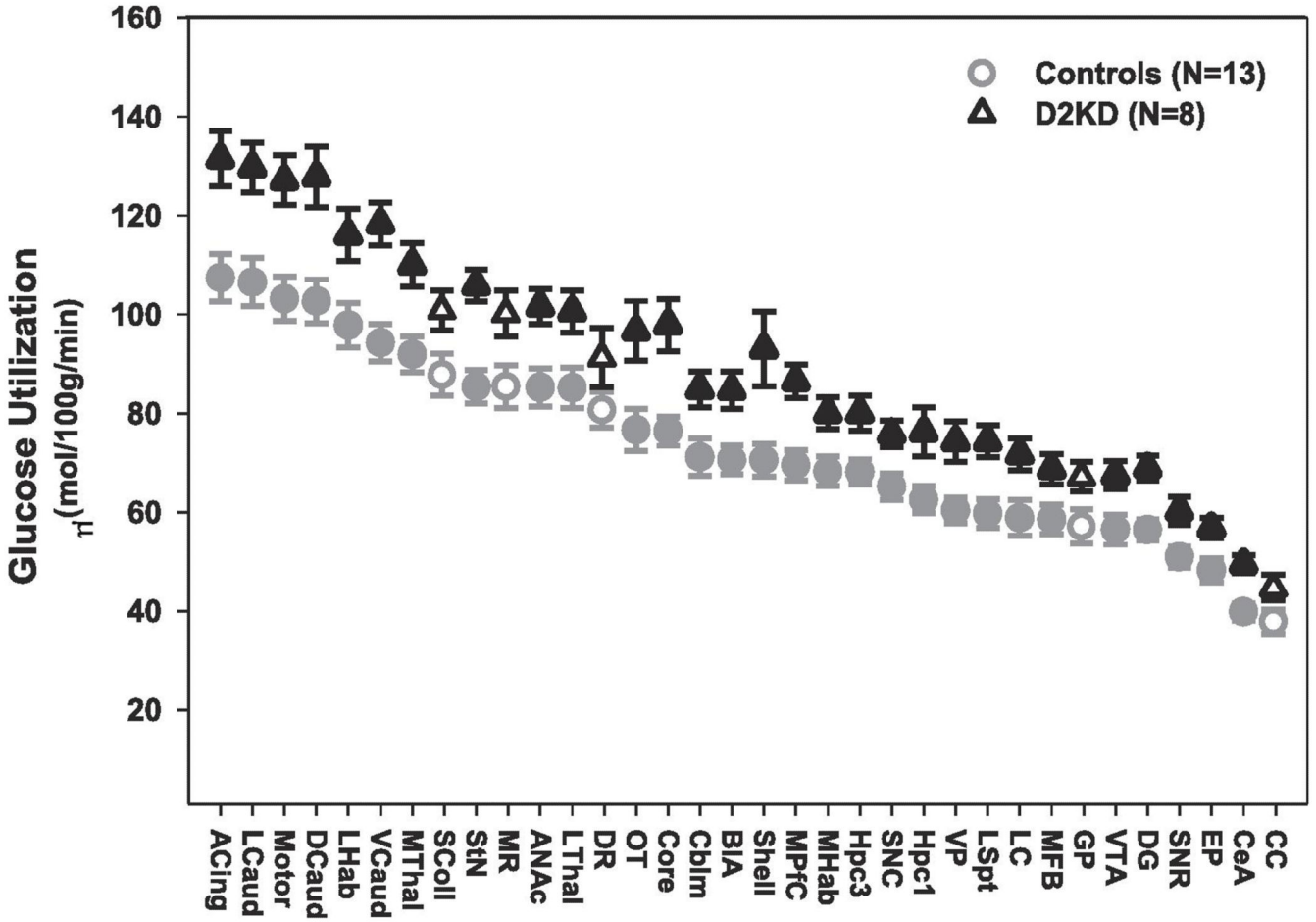

Figure 2.

Average glucose utilization for *Drd2* knockdown and control animals across 34 brain regions. Brain regions represented by filled symbols were significantly different from control at $p < .025$. Brain regions represented by open symbols were not found to be significant at $p < .025$. Abbreviations: ACing, Anterior Cingulate; ANAc, Anterior Nucleus Accumbens; BlA, Basolateral Amygdala; Cblm, Cerebellum; CC, Corpus Callosum; CeA, Central Amygdala; Core, Nucleus Accumbens Core; DCaud, Dorsal Caudate; DG, Dentate Gyrus; DR, Dorsal Raphe Nucleus; EP, Entopeduncular Nucleus; GP, Globus Pallidus; Hpc1, Hippocampus CA1; Hpc3, Hippocampus CA3; LC, Locus Coeruleus; LCaud, Lateral Caudate; LHab, Lateral Habenula; LSpt, Lateral Septum; LThal, Lateral Thalamus; MFB, Medial Forebrain Bundle; MHab, Medial Habenula; Motor, Motor Cortex, MPfC, Medial Prefrontal Cortex; MR, Medial Raphe Nucleus; MThal, Medial Thalamus; OT, Olfactory Tubercle; SColl, Superior Colliculus; Shell, Nucleus Accumbens Shell; SNC, Substantia Nigra Compacta; SNR, Substantia Nigra Reticulata; StN, Subthalamic Nuclei; VCaud, Ventral Caudate; VP, Ventral Pallidum; VTA, Ventral Tegmental Area

Table 1.

Effects of VTA *Drd2* mRNA knockdown on rates of local cerebral glucose utilization in rat brain

	Controls		Treated
Brain Region	**PBS (N=5)**	**SCR (N=8)**	***Drd2*KD (N=8)**
Mesolimbic			
Rostral accumbens	89.0 ± 7.4	82.9 ± 4.0	101.6 ± 3.6 **
Accumbens core	79.0 ± 5.1	77.4 ± 3.5	97.9 ± 5.3 **
Accumbens shell	71.8 ± 4.9	69.8 ± 4.3	93.0 ± 7.6 **
Olfactory tubercle	77.4 ± 7.0	76.2 ± 5.5	96.6 ± 6.0 *
Ventral pallidum	64.8 ± 4.0	57.7 ± 3.0	74.3 ± 4.1 *
Ventral tegmental area	59.2 ± 3.8	54.7 ± 4.2	67.6 ± 2.8 *
Lateral habenula	97.9 ± 6.6	97.8 ± 6.0	116.1 ± 5.3 *
Nigrostriatal			
Dorsal caudate	106.4 ± 7.1	100.3 ± 5.5	127.8 ± 6.2 **
Lateral caudate	111.4 ± 7.8	103.5 ± 6.1	129.7 ± 5.1 **
Ventral caudate	102.5 ± 5.1	99.1 ± 4.3	118.3 ± 4.3 **
Globus pallidus	63.2 ± 4.4	53.1 ± 4.3	67.0 ± 3.0
Entopeduncular nucleus	48.9 ± 3.3	47.7 ± 3.3	56.8 ± 2.1 **
Subthalamic nucleus	83.9 ± 5.3	86.3 ± 4.4	105.8 ± 3.2 **
Substantia nigra compacta	68.4 ± 3.7	63.2 ± 3.5	75.9 ± 2.7 *
Substantia nigra reticulata	50.4 ± 3.6	51.2 ± 2.7	60.3 ± 2.9 **
Limbic			
Lateral septum	61.9 ± 5.5	58.4 ± 3.3	74.3 ± 3.2 **
Medial forebrain bundle	58.9 ± 4.4	58.4 ± 4.1	68.7 ± 3.1 *
Basolateral amygdala	72.0 ± 4.9	69.8 ± 3.7	84.6 ± 3.7 **
Central amygdala	40.9 ± 2.7	39.2 ± 2.2	49.5 ± 1.8 **
Hippocampus CA1	63.3 ± 4.4	62.1 ± 3.5	76.2 ± 4.9 *
Hippocampus CA3	66.9 ± 4.6	69.0 ± 3.0	80.0 ± 3.5 *
Dentate gyrus	54.6 ± 2.5	57.6 ± 3.0	68 9 ± 2.5 **
Cortex and Thalamus			
Medial prefrontal cortex	71.9 ± 5.7	68.0 ± 3.5	86.5 ± 3.4 **
Anterior cingulate	110.2 ± 8.3	105.7 ± 5.9	131.5 ± 5.5 **
Motor cortex	101.4 ± 7.4	102.4 ± 5.7	127.1 ± 5.1 **
Corpus callosum	38.7 ± 4.3	37.0 ± 2.9	44.5 ± 2.6
Lateral thalamus	81.2 ± 6.7	87.6 ± 5.0	100.6 ± 4.3 *
Medial thalamus	91.4 ± 5.0	92.2 ± 4.9	110.0 ± 4.4 **
Habenula	66.5 ± 4.3	69.4 ± 4.0	80.0 ± 3.3 *

	Controls		Treated
Brain Region	**PBS (N=5)**	**SCR (N=8)**	***Drd2*KD (N=8)**
Brainstem			
Superior colliculus	91.3 ± 5.7	85.3 ± 5.7	100.6 ± 4.0
Dorsal raphe	80.7 ± 6.5	80.4 ± 4.2	91.1 ± 6.0
Median raphe	89.4 ± 5.9	82.7 ± 5.8	100.0 ± 4.6
Locus coeruleus	59.1 ± 5.9	58.7 ± 4.7	71.7 ± 3.3 *
Cerebellum	72.2 ± 6.4	70.5 ± 4.7	84.9 ± 3.7 *

Data are expressed as mean (μmol/100 g/ min) ± S.E.M.

* $p < .025$,

** $p < .010$ compared to combined control groups